Water Research 135 (2018) 1–10

Contents lists available at ScienceDirect

Water Research

journal homepage: www.elsevier.com/locate/watres

Factors influencing degradation of trichloroethylene by sulfide-modified nanoscale zero-valent iron in aqueous solution

Haoran Dong [a, b, *], Cong Zhang [a, b], Junmin Deng [a, b], Zhao Jiang [a, b], Lihua Zhang [a, b], Yujun Cheng [a, b], Kunjie Hou [a, b], Lin Tang [a, b], Guangming Zeng [a, b]

[a] College of Environmental Science and Engineering, Hunan University, Changsha, Hunan 410082, China
[b] Key Laboratory of Environmental Biology and Pollution Control (Hunan University), Ministry of Education, Changsha, Hunan 410082, China

ARTICLE INFO

Article history:
Received 10 August 2017
Received in revised form
1 February 2018
Accepted 7 February 2018
Available online 7 February 2018

Keywords:
Sulfidation
Nanoscale zero-valent iron
Ferrous sulfide
Dechlorination
TCE

ABSTRACT

Sulfide-modified nanoscale zero-valent iron (S/NZVI) has been considered as an efficient material to degrade trichloroethylene (TCE) in groundwater. However, some critical factors influencing the dechlorination of TCE by S/NZVI have not been investigated clearly. In this study, the effects of Fe/S molar ratio, initial pH, dissolved oxygen and particle aging on TCE dechlorination by S/NZVI (using dithionite as sulfidation reagent) were studied. Besides, the feasibility of reactivation of the aged-NZVI by sulfidation treatment was looked into. The results show that the Fe/S molar ratio and initial pH significantly influenced the TCE dechlorination, and a higher TCE dechlorination was observed at Fe/S molar ratio of ~60 under alkaline condition. Spectroscopic analyses demonstrate that the enhanced TCE dechlorination was associated with the presence of FeS on the surface of S/NZVI. Dissolved oxygen had little effect on TCE dechlorination by S/NZVI, revealing that the FeS layer could be able to alleviate the surface passivation of NZVI caused by oxidation. Aging of S/NZVI up to 10–20 d only slightly decreased the dechlorination efficiency of TCE. Although an obvious drop in dechorination efficiency was observed for the S/NZVI aged for 30 d, it still exhibited a higher reactivity than the bare NZVI. This indicates that sulfidation of NZVI did prolong its lifetime. Additionally, sulfidation treatment was used to reactivate the aged NZVI, and the results show that the reactivated NZVI even had higher reactivity than the fresh NZVI, suggesting that sulfidation treatment would be a promising method to reactivate the aged NZVI.

1. Introduction

Chlorinated hydrocarbons have been widely used in industrial production (Seyama et al., 2012; Wei and Seo, 2010). Accidental leakage and improper disposal of the chlorinated hydrocarbons have resulted in serious groundwater contamination (Stroo et al., 2003; Dong et al., 2017a). Trichloroethene (TCE) is one of the most commonly detected chlorinated hydrocarbons in groundwater. TCE, a type of potent carcinogen, is persistent to natural degradation (Yan et al., 2015; Dong et al., 2017b). Cleanup of TCE-contaminated groundwater has been a challenging task for decades.

To remove TCE from groundwater, various methods have been employed, including biological reductive dechlorination (Shao and Butler, 2009), physical adsorption (Ahmad et al., 2012; Wei and Seo, 2010), chemical reduction (Gao et al., 2015; Wang and Zhang, 1997) and oxidation (Weir et al., 2010; Yan et al., 2015). Among those methods, nanoscale zero-valent iron (NZVI)-induced chemical reduction has been considered as a promising technique to remediate groundwater contaminated by TCE. NZVI can eventually dechlorinate TCE into non-toxic products while releasing chloride ions (Arnold and Roberts, 2000; Chen et al., 2001), which was mainly based on the reduction of TCE by Fe^0 and Fe^{2+} on the surface of NZVI. In spite of the high reactivity of NZVI, corrosion of iron in aqueous solutions may cause surface passivation, thus decreasing its reactivity (Liang et al., 2014; Dong et al., 2016a, 2017c; Qin et al., 2017; Xie et al., 2017). Recently, some studies have reported the reactivity of NZVI towards chlorinated contaminants was enhanced in the presence of sulfur compounds (Kim et al., 2013; Rajajayavel and Ghoshal, 2015; Han and Yan, 2016). The sulfide-modified NZVI (S/NZVI) has been synthesized to degrade TCE and yielded a better dechlorination efficiency than NZVI (Kim et al., 2013;

* Corresponding author. College of Environmental Science and Engineering, Hunan University, Changsha, Hunan 410082, China.
E-mail address: dongh@hnu.edu.cn (H. Dong).

https://doi.org/10.1016/j.watres.2018.02.017
0043-1354/

Rajajayavel and Ghoshal, 2015). As for the reason for the enhanced dechlorination efficiency caused by the sulfide modification, researchers have not reached a consensus yet. Some mechanisms were proposed, including more efficient electron transfer mediated by the iron sulfide layer (Rajajayavel and Ghoshal, 2015), improved contaminant-specific property (selective against the background reaction of water reduction) of S/NZVI (Han and Yan, 2016), increased depassivation of iron surface (Hansson et al., 2008). The different mechanisms might result from the difference in experiment conditions (e.g., type of sulfidation reagent, molar ratio of Fe/S). Han and Yan (2016) reported that the reactivity of sulfur-treated NZVI was unaffected by the sulfidation reagent (i.e., sodium sulfide, dithionite, and thiosulfate), but was dependent strongly on the molar ratio of Fe/S. However, in regard to the effect of Fe/S molar ratio, different findings were reported (Kim et al., 2011; Rajajayavel and Ghoshal, 2015; Han and Yan, 2016). Kim et al. (2011) found that the Fe/FeS nanoparticles had a higher reactivity towards TCE than the unamended NZVI, and the enhancements in reactivity were relatively constant over a large range of dithionite doses. The study of Rajajayavel and Ghoshal (2015), however, reported that Fe/S ratios in the range of 12–25 provided the highest TCE dechlorination rates, and rates decreased at both higher and lower Fe/S ratio. Different from both the above two studies, Han and Yan (2016) reported that TCE degradation was accelerated with increasing sulfur dose at a low sulfur loading but the rate constant reached a constant value as the Fe/S ratio was lower than 40. Accordingly, the effect of Fe/S molar ratio on TCE degardation and the underlying mechanisms need to be further investigated.

Moreover, some other critical factors which might influence the reactivity of S/NZVI (e.g., pH, dissolved oxygen, particle aging) are not well studied in previous studies and need to be further identified. These factors have been reported to significantly influence the corrosion process and thus the reactivity of bare NZVI (Dong et al., 2016b), thus, a comparison study on the influences of these factors on the reactivity of S/NZVI and bare NZVI is essential to better understand the underlying mechanisms of the enhanced reactivity of S/NZVI. Yet, no studies have systematically compared the reactivity of S/NZVI and NZVI under the varying conditions.

The objectives of this study were to assess the influences of the molar ratio of Fe/S, solution pH, dissolved oxygen and aging time of particles on the removal efficiency and dechlorination efficiency of TCE by S/NZVI. Besides, we also attempted to verify whether sodium dithionite ($Na_2S_2O_4$) could reactivate the aged NZVI for the dechlorination of TCE. To probe into the mechanism of TCE dechlorination by S/NZVI, Transmission electron microscopy and energy dispersive spectroscopy (TEM-EDS), Fourier transform infrared spectroscopy, X-ray diffraction (XRD) and X-ray photoelectron spectroscopy (XPS) analysis were carried out to characterize the physicochemical properties of S/NZVI.

2. Experimental section

2.1. Reagents

Iron(III) chloride hexahydrate ($FeCl_3 \cdot 6H_2O$, analytical reagent grade (AR)), sodium borohydride ($NaBH_4$, AR) used for synthesis of NZVI and S/NZVI were purchased from Sinopharm Chemical Reagent Co., Ltd, China. Sodium dithionite ($Na_2S_2O_4$, AR) used for sulfurating NZVI were purchased from Xilong Scientific Co., Ltd, China. Hexane (HPLC) used as extractant for TCE detection was purchased from Tianjin chemical reagent research institute co., Ltd, China. TCE (AR) was purchased from Huihong reagent co., Ltd, China.

2.2. Synthesis of NZVI and S/NZVI

The bare NZVI was synthesized according to the borohydride reduction method (Khalil et al., 2016; Liu et al., 2005). The synthesis of S/NZVI was following a method as described by Kim et al. (2011). Firstly, the $FeCl_3 \cdot 6H_2O$ (0.05 M) solution was prepared and purged with N_2 for at least 30 min to create an anoxic environment (dissolved oxygen < 0.2 mg/L). Then a mixture of $NaBH_4$ (0.2 M) and $Na_2S_2O_4$ solution was prepared and added drop-wisely into the $FeCl_3 \cdot 6H_2O$ solution, followed by 30 min of mechanical stirring. The dosage of $Na_2S_2O_4$ was varied in the synthesis mixture such that the Fe/S molar ratio changed in the range of 10–100. The resulting NZVI or S/NZVI suspension was washed at least 3 times with deionized water and ethanol, and dried in a vacuum drying oven at 60 °C for 8 h. The dry particles were stored in sealing films at a low temperature, and used in batch experiments within 3 d.

2.3. Characterization of NZVI and S/NZVI

Transmission electron microscopy (TEM, JEOL-2010) and energy dispersive spectroscopy (EDS) analyzers were employed to investigate the structure and surface atomic distribution of nanoparticles. Fourier transform infrared spectroscopy (FTIR, Magna-IR 750, Nicolet) analysis were carried out to explore sulfur compounds on the particle surface of S/NZVI. Spectra were collected over the range 4000–500 cm^{-1}. X-ray photoelectron spectrometry (XPS, Thermo ESCALAB 250XI, Thermo Fisher Scientific) was used to analyze the surface composition of the nanoparticles. The samples were irradiated using a monochrome Al Kα (hν = 1486.6 eV) source at a power of 150 W. The binding energy was calibrated with C 1s peaks at 284.8 eV. The narrow scans over the selected binding energy range of 158.45–176.45 eV, 701.45–741.45 eV, and 180.45–299.45 eV were used to identify and analyze elemental valence of sulfur, iron, and carbon, respectively. XRD analysis was conducted to identify the aging products of NZVI or S/NZVI particles using a Rigaku D/Max 2500 with Cu-Kα radiation at 40 kV/250 mA (2θ range 10–90).

2.4. Batch experiments

Batch experiments were performed to compare the removal efficiency and dechlorination efficiency (i.e. the molar ratio of Cl^- in solution to that in initial TCE) of TCE by S/NZVI under various conditions. The initial pH (pH = 5.57, 7.10 and 8.02) of solutions was adjusted using dilute NaOH or HCl. The samples were prepared in 40-mL glass vials containing 20 mL solution. 100 mg dry particles were added into the vials to reach a particle concentration of 5 g/L. Then, a certain volume of TCE stock solution dissolved in methanol was injected into the vials to prepare TCE with initial concentration of 30 mg/L. The vials were transferred to a horizontal shaker at 250 rpm at 20 ± 2 °C. Aqueous suspensions were periodically sampled from the glass vials, and filtered through 0.45-μm needle filter. Then the TCE in aqueous phase were extracted with chromatographically pure n-hexane, and analyzed using a Gas Chromatograph-Flame Ionization Detector (GC-FID) equipped with a DB-624 capillary column (30 m × 0.53 mm × 3 μm). Simultaneously, the concentration of Cl^- in aqueous solution was detected with UV spectrophotometer (UV-2550, SHIMADZU, Japan) (Utsumi, 2006). To differentiate the two possible ways (adsorption and degradation) of TCE removal from aqueous solution, the total residual TCE (i.e., both in aqueous phase and solid phase) in the sample was extracted by addition of pure n-hexane. Then the portion of TCE adsorbed onto the particle surface was obtained by subtraction of TCE concentration in aqueous phase from the total residual TCE concentration, and the portion of degraded TCE was

determined by the subtraction of the adsorbed TCE from the total removed TCE.

To assess the effect of aging time on TCE removal by S/NZVI, 100 mg S/NZVI particles and 20 mL deoxygenated deionized water were added into the 40-mL vial. Then the vials were sealed and placed in dark room for aging. At determined time intervals (10 d, 20 d and 30 d), the aged samples were collected and used for TCE removal following the same procedure as described above.

In the experiment of reactivation of the aged NZVI by $Na_2S_2O_4$, the NZVI particles were exposed to air and aged naturally for different time. Then the aged NZVI was reactivated by $Na_2S_2O_4$ following a similar procedure as the synthesis of S/NZVI. Briefly, 1 g aged NZVI particles were added into a three-necked flask with 714 mL deionized water. The solution was degassed with N_2 for at least 30 min to achieve an anoxic environment. 522 μL $Na_2S_2O_4$ solution (100 g/L) was dropped into the flask (the theoretical ratio of Fe/S was 60), followed by 30 min of mechanical stirring. Then the treated particles were collected and used for TCE removal following the same procedure as described above.

All experiments were performed in triplicate to ensure that reproducible results were obtained. The data reported here were the average of three replicated experiments and error bars represent the standard deviation of the averages.

3. Results and discussion

3.1. Effect of Fe/S molar ratio on TCE removal by S/NZVI

S/NZVI particles synthesized at different molar ratios of Fe/S (ranging from 100 to 10) were used for TCE removal and the results are shown in Fig. 1A. It was found that the molar ratio of Fe/S had a significant effect on the removal of TCE by S/NZVI. On the whole, the sulfidation of NZVI greatly increased the removal efficiency of TCE compared with the bare NZVI. However, the removal rate of TCE differed for S/NZVI synthesized at different molar ratios of Fe/S. It was found that S/NZVI (Fe/S = 60) provided the highest TCE removal efficiency which decreased at both higher and lower Fe/S. Our observed trends on the effects of sulfide concentration on reactivity were similar to that of Rajajayavel and Ghoshal (2015). Han and Yan (2016) also reported the rate of TCE degradation by S/NZVI was accelerated with increasing sulfur dose at a low sulfur loading, but the rate constant reached a limiting value and kept constant rather than decreasing with further increase of sulfur loading.

Given that the removal efficiency might not represent the degradation efficiency of TCE by S/NZVI, the dechlorination efficiency was further studied at selected Fe/S molar ratios (i.e., 10, 60 and 100). The concentration of chloride ions generated in the solution was examined, and the theoretical dechlorination efficiency was shown in Fig. 1B. In general, the dechlorination efficiency of TCE by S/NZVI was much higher than that of bare NZVI. When increasing the dosage of sulfur, the dechlorination increased to a maximum value at Fe/S ratio of 60, and then decreased, which shows the same trend as that observed in the removal efficiency of TCE (as demonstrated in Fig. 1A). However, it was found that even though the removal efficiency of TCE reached nearly 100% after 9-h reaction at Fe/S molar ratio of 60, the dechlorination efficiency was only around 35%. This indicates that TCE was only partially degraded or adsorbed onto the surface of S/NZVI particles. Then, the proportion of TCE by degradation and adsorption was further determined (Fig. 1C). The results show that the TCE degradation by bare NZVI was trivial within 9-h reaction, and the removal of TCE by NZVI was mainly due to adsorption. This is consistent with the previous studies (Wang and Zhang, 1997; Liu et al., 2005; Dong et al., 2017a), in which it was reported that the reaction rate of bare NZVI with TCE was slow and the degradation occurred only after several days of reaction. The results further verified that the sulfidation of NZVI significantly enhanced the degradation of TCE, and the optimum degradation efficiency was observed at Fe/S molar ratio of 60 (Fig. 1C).

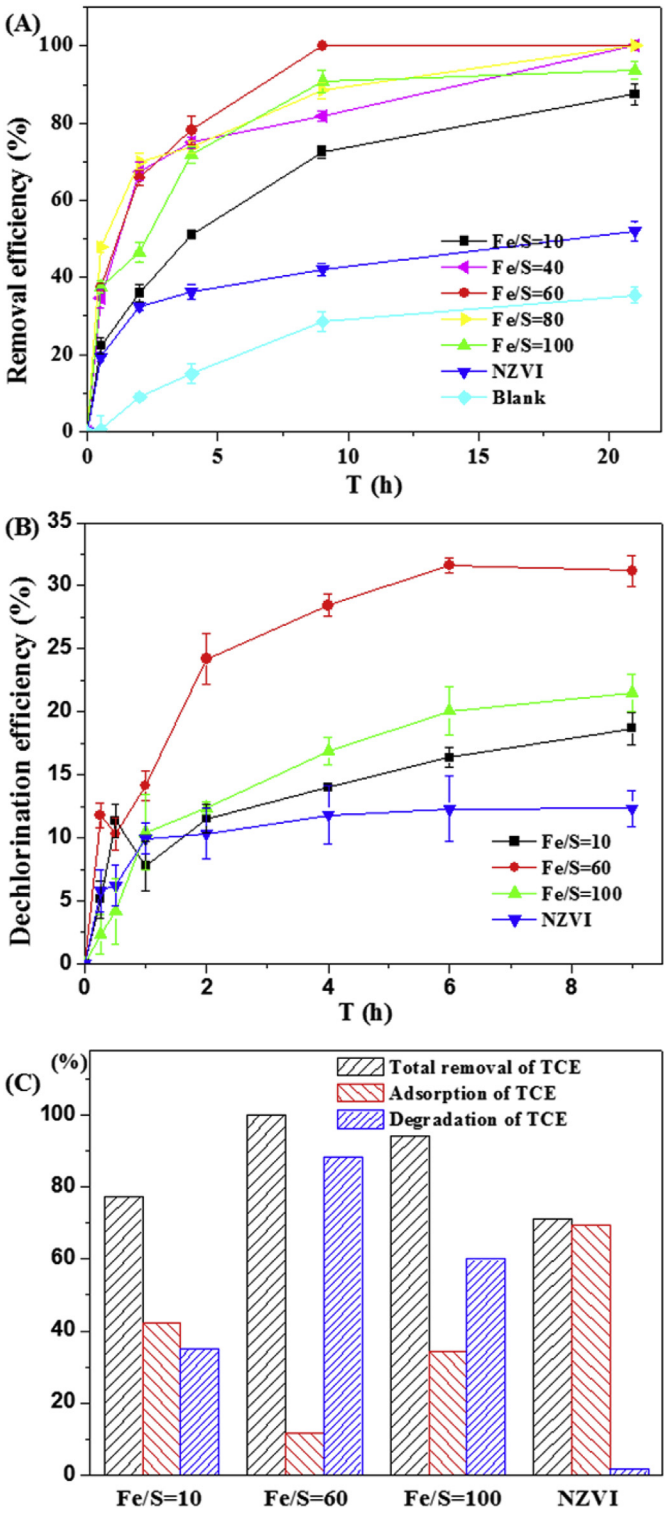

Fig. 1. Effect of Fe/S molar ratio on (A) total removal of TCE within 22 h, (B) dechlorination of TCE within 9 h, and (C) total removal/adsorption/degradation of TCE within 9 h by S/NZVI. (TCE = 30 mg/L, NZVI=S/NZVI = 5 g/L, pH = 5.57).

Previous studies have reported that the enhanced reactivity of NZVI by sulfidation should be ascribed to the formation of FeS_x layer on the surface of NZVI (Rajajayavel and Ghoshal, 2015; Han and Yan, 2016). Thus, given the different performance of TCE degradation by S/NZVI prepared at different Fe/S molar ratios in this study, it was suspected that different Fe-S compounds might be formed on the surface of NZVI at different Fe/S molar ratios.

In the synthesis process of S/NZVI, the decomposition of $S_2O_4^{2-}$ could produce a variety of sulfur species (Eqs. (1)–(6)) (Garcia et al., 2016; Han and Yan, 2016). Among such sulfur species, the presence of sulfide (S^{2-}) or elemental sulfur (S^0) would contribute to the formation of FeS on the surface of Fe^0 (Eqs. (7)–(9)), which could promote the dechlorination of TCE (Rajajayavel and Ghoshal, 2015; Han and Yan, 2016). Nevertheless, the excessive amount of sulfur might generate polysulfide compounds (S_n^{2-}), which has a lower reactivity towards TCE compared with FeS (Garcia et al., 2016; Han and Yan, 2016). Meanwhile, the excessive $S_2O_4^{2-}$ might be decomposed into sulfite (SO_3^{2-}) and sulfate (SO_4^{2-}) (Eqs. (1)–(3)), the salts of which would deposit onto the surface of Fe^0 and then influence the electron transfer between Fe^0 and TCE (Garcia et al., 2016).

$$2S_2O_4^{2-} + H_2O \rightarrow 2SO_3^{2-} + S_2O_3^{2-} + 2H^+ \quad (1)$$

$$2SO_3^{2-} + H_2O \rightarrow 2SO_4^{2-} + 4e^- + 4H^+ \quad (2)$$

$$S_2O_3^{2-} + 5H_2O \rightarrow 2SO_4^{2-} + 8e^- + 10H^+ \quad (3)$$

$$S_2O_3^{2-} \rightarrow SO_3^{2-} + S^0 \quad (4)$$

$$S_2O_4^{2-} + S_2O_3^{2-} + 2H_2O + H^+ \rightarrow 3HSO_3^- + H_2S \quad (5)$$

$$H_2S \rightarrow S^{2-} + 2H^+ \quad (6)$$

$$Fe^0 + 2H_2O \rightarrow Fe^{2+} + H_2 + 2OH^- \quad (7)$$

$$Fe^0 + S^0 \rightarrow FeS \quad (8)$$

$$S^{2-} + Fe^{2+} \rightarrow FeS \quad (9)$$

To elucidate the physicochemical properties of S/NZVI, spectroscopic analysis were performed on the three types of S/NZVI (prepared at Fe/S molar ratios of 100, 60 and 10).

S/NZVI and NZVI samples were characterized using TEM coupled with EDS for comparison. Fig. S1 shows NZVI particles with primary particle diameters ~10–20 nm are aggregated in chain structures. Fig. 2A–C shows TEM images of S/NZVI at Fe/S molar ratios of 100, 60 and 10. It was found that aggregation of S/NZVI is not as significant as NZVI, which might be due to the reason that the FeS_x coating decreases magnetic attractions between the particles (Su et al., 2015). It was also observed that S/NZVI has different particle size and morphology compared to NZVI. The particle size of S/NZVI increases with the decreasing Fe/S molar ratio, which is ~50 nm, ~100 nm and ~200 nm at Fe/S molar ratios of 100, 60 and 10, respectively. S/NZVI has a flake-like shell and the level of flaking increases with decreasing Fe/S ratio. The 'flake-like shell' was also observed by Su et al. (2015), who reported that S/NZVI has much higher surface to volume ratio due to the abundant flake-like structure, compared with NZVI. Thus, the decreased aggregation and the higher surface to volume ratio might contribute to the enhanced reactivity of S/NZVI. The EDS, however, showed only Fe and O as the main elements with no or very low levels of sulfur (Fig. S2). This phenomenon was also observed by Fan et al. (2014). It is possible that these structures on the surface of S/NZVI were some transient phases of FeS oxidation and had yet to be transformed to more stable phases.

To verify the formation of sulfur compounds on the surface of S/NZVI as illustrated in Eqs. (1)–(9), FTIR spectra of NZVI and S/NZVI were collected for comparison (Fig. 3). The broad band appeared at ~3400 cm^{-1} could come from hydroxyl groups of lattice water. The peak at around ~2350 cm^{-1} should be assigned to the saturation band of CO_2. The bands at ~1630 cm^{-1} and ~1450 cm^{-1} can be attributed to the asymmetric and symmetric stretching vibrations of C=O (Dong et al., 2016b). The above bands existed in both NZVI and S/NZVI samples. However, some new bands appeared at ~1100 cm^{-1} and 920 cm^{-1} for S/NZVI samples, which could be assigned to the presence of SO_4^{2-}, $S_2O_3^{2-}$ or SO_3^{2-} (Chernyshova, 2003; Reyes-Bozo et al., 2015). This verified the mechanisms proposed in Eqs. (1)–(4). The bands observed at lower wavenumbers between ~620 cm^{-1} and 500 cm^{-1} could be assigned to the typical Fe-O and Fe-S bonds (Dong et al., 2016b; Reyes-Bozo et al., 2015). However, as demonstrated in Fig. 3, it is difficult to differentiate the iron oxides and iron sulfide (FeS_x).

To further clarify the exact Fe-S compounds formed on the surface of S/NZVI, XPS analysis were carried out (Fig. 4). Fig. 4A shows the high resolution XPS for the S 2p region. For S/NZVI, the $2p_{3/2}$ peaks for sulfide (S^{2-}) and polysulfide (S_n^{2-}) were detected at 161.7 eV and 162.6 eV, respectively (Garcia et al., 2016). For S/NZVI with Fe/S molar ratio of 100, the contents of sulfide and polysulfide were low, but obviously the content of sulfide was much higher than that of polysulfide. The content of sulfide and polysulfide increased with the increasing dosage of $S_2O_4^{2-}$, and the content of polysulfide was similar to that of sulfide for S/NZVI with Fe/S molar

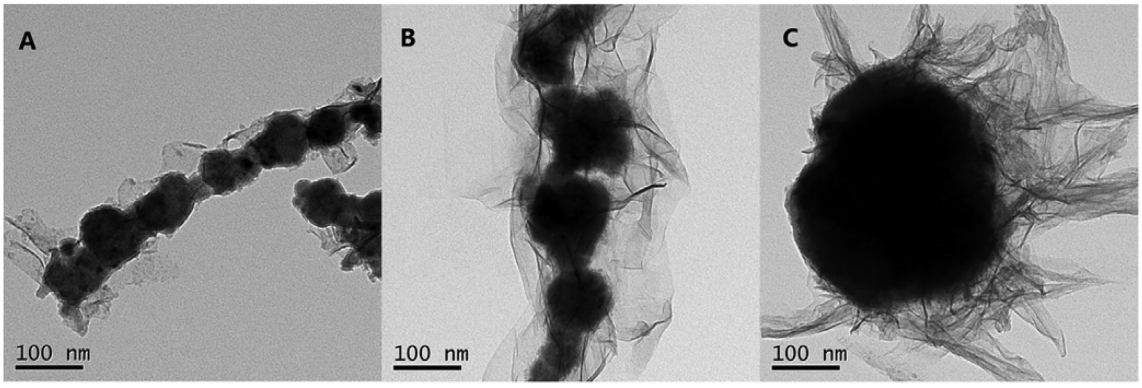

Fig. 2. TEM images of S/NZVI synthesized at different Fe/S molar ratios: (A) Fe/S = 100; (B) Fe/S = 60; (C) Fe/S = 10.

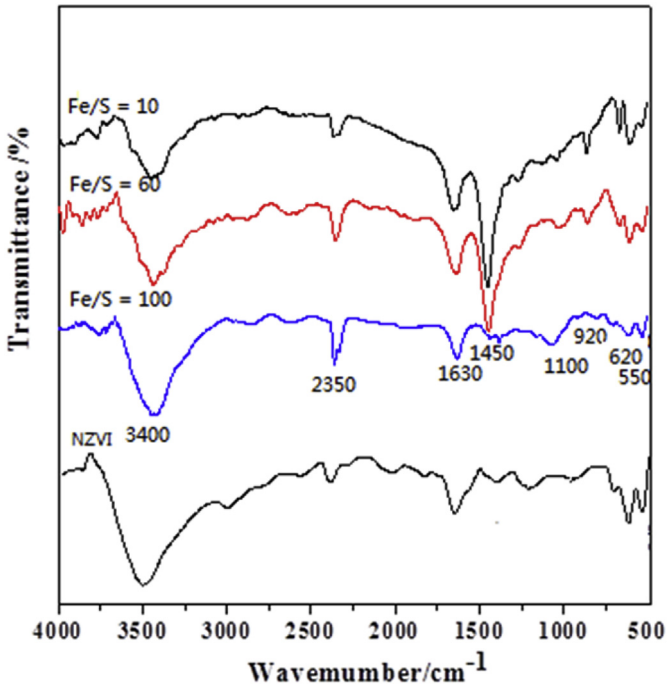

Fig. 3. FTIR analysis of NZVI and S/NZVI synthesized at different Fe/S molar ratios.

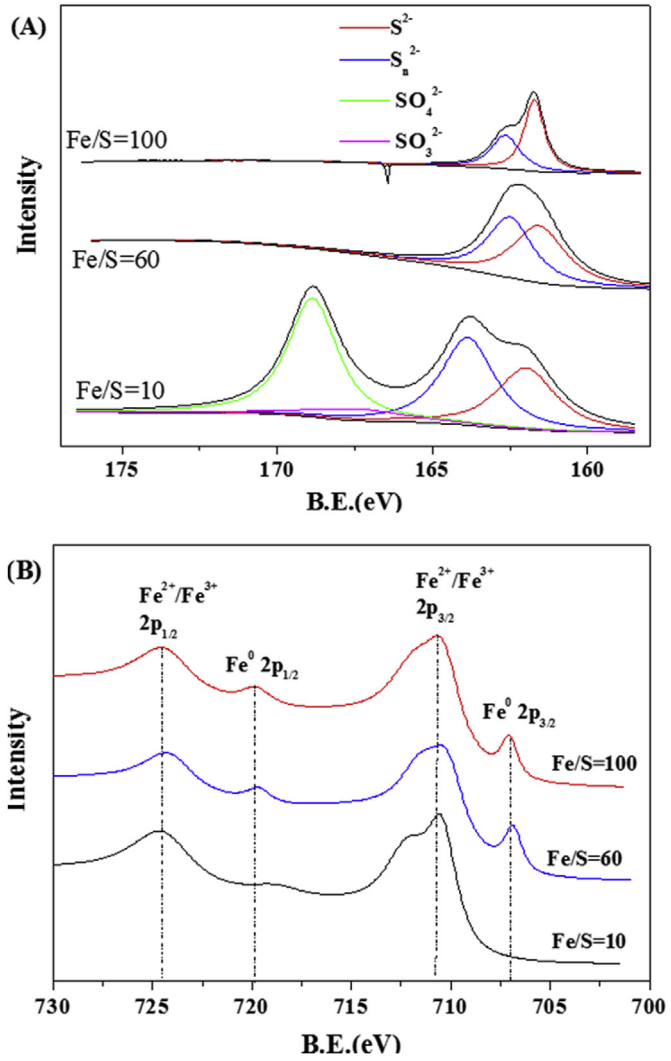

Fig. 4. High resolution XPS for the S 2p region (A) and Fe 2p region (B).

ratio of 60. When the dosage of $S_2O_4^{2-}$ was further increased, sulfide content increased slightly while polysulfide content increased markedly. Simultaneously, a small peak of sulfite (SO_3^{2-}) and a pronounced peak of sulfate (SO_4^{2-}) were detected at 167.4 eV and 168.9 eV, respectively (Garcia et al., 2016).

Due to the addition of $S_2O_4^{2-}$, Fe^0 would convert into iron with different valences, and the content of Fe^0 could indirectly reflect the reducing capacity of S/NZVI. Therefore, the high resolution XPS for the Fe 2p region was detected and shown in Fig. 4B. The broad peaks of Fe 2p1/2 (~723 eV) and Fe 2p3/2 (~710 eV) account for the oxidized iron species (Fe^{2+} and Fe^{3+}) (Yamashita and Hayes, 2008; Jeong et al., 2010; Garcia et al., 2016), which are predominant in all the three types of S/NZVI particles. The satellite peak obtained at ~714 eV was assigned to Fe 2p3/2 of Fe^{2+} (Yamashita and Hayes, 2008). The oxidized iron for these nanoparticles could be present as iron oxides, oxyhydroxides, hydroxides, and sulfides. The peaks of Fe^0 $2p_{3/2}$ (~707eV) and Fe^0 $2p_{1/2}$ (~719eV) account for less proportion, indicating that the oxidized iron species were dominant on the surface of S/NZVI. When the Fe/S molar ratio was 10, the peaks representing Fe^0 even disappeared. It could be speculated that the large portion of Fe^0 was oxidized with the addition of $S_2O_4^{2-}$ in the synthesis process, generating iron oxide or Fe-S compounds.

The above XPS analysis indicates that FeS was generated on the surface of NZVI at lower dosage of $S_2O_4^{2-}$, while large amounts of FeS_2 and SO_4^{2-} accumulated on the surface of NZVI at higher dosage of $S_2O_4^{2-}$. Although the presence of FeS could enhance the reactivity of Fe^0 (Rajajayavel and Ghoshal, 2015), FeS_2 has a much lower reactivity towards TCE than FeS (Lee and Batchelor, 2002). Meanwhile, at higher dosage of $S_2O_4^{2-}$, Fe^0 content decreased significantly and a large amount of sulfate were deposited onto the particle surface, which reduced the electron donor and also hindered the transfer of electrons. Accordingly, the enhanced degradation of TCE by S/NZVI at higher molar ratio of Fe/S (from 100 to 60) should be due to the presence of FeS, while the inhibited TCE degradation at lower molar ratio of Fe/S (from 60 to 10) should be due to the accumulation of FeS_2, sulfate and iron oxides on the surface of S/NZVI, and the consumption of Fe^0.

3.2. Effect of pH

It is known that the reactivity of NZVI is greatly susceptible to solution pH. Under alkaline conditions, NZVI has a lower reactivity due to surface passivation, while under acidic conditions, NZVI has a higher reactivity due to rapid corrosion (Matheson and Tratnyek, 1994). However, the Fe/S layer formed on the surface of NZVI via sulfidation was reported to be able to enhance electron transfer and increase depassivation of NZVI (Hansson et al., 2008; Rajajayavel and Ghoshal, 2015; Han and Yan, 2016), which might exert some different effects on the removal of TCE by S/NZVI at different pH. Therefore, the effect of initial pH on the removal of TCE by S/NZVI was studied (Fig. 5). It was found that the removal of TCE by S/NZVI was slightly affected by pH value, all of which could reach 90% after 9 h of reaction (Fig. 5A). The trend of TCE removal with pH seems to be contrary to the previous literature (Kim et al., 2013; Rajajayavel and Ghoshal, 2015), in which the increasing solution pH could significantly increase TCE degradation. However, as discussed in our previous section, the TCE removal in this study could result from both degardation and adsorption, which might give rise to the differences in pH-dependent trend from other studies that only

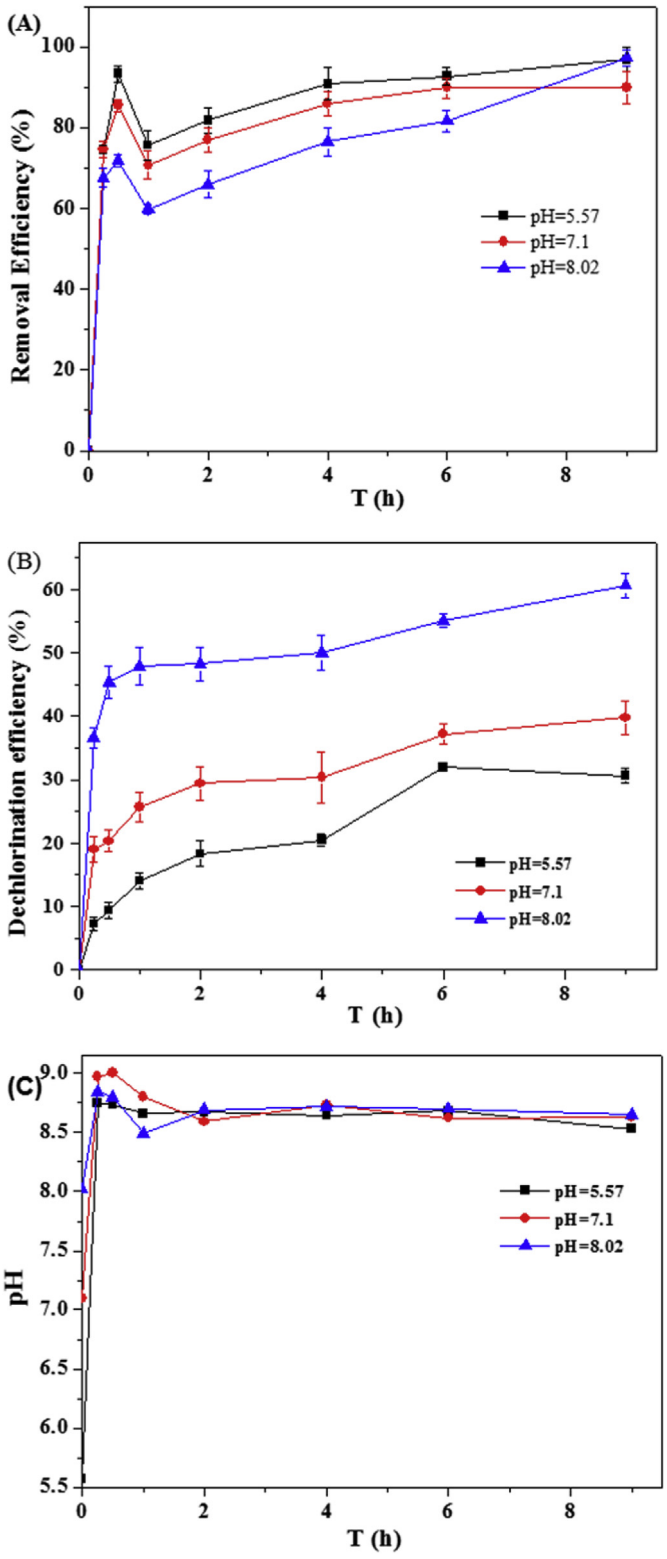

Fig. 5. Effect of pH on (A) TCE removal and (B) TCE dechlorination by S/NZVI, and (C) the variation of pH during the reaction. (Fe/S = 60; TCE = 30 mg/L; S/NZVI = 5 g/L).

take degardation into account. Thus, the degradation of TCE with pH was further examined by determining the dechlorination efficiency (Fig. 5B). As shown in Fig. 5B, the dechlorination efficiency increased significantly with increase of pH value. The dechlorination efficiency merely achieved 31.5% at initial pH 5.57, while it could reach up to 60.7% at initial pH 8.02. The trend of TCE degradation with pH is consistent with the pH effect observed in iron sulfide systems reported previously, but opposite to that in the single NZVI systems (Butler and Hayes, 2001; Kim et al., 2013; Rajajayavel and Ghoshal, 2015). In order to further explore the role of pH played on the TCE degradation process, the variation of pH with reaction time was monitored (Fig. 5C). Although there was a great difference in the initial pH (from 5.57 to 8.02) of the three samples, the pH of solution became similar after reaction for just a few minutes. The final pH increased to around 8.5 in all three samples. This indicates that the initial pH plays a more important role in the dechlorination of TCE by S/NZVI. As shown in Fig. 5C, the initial pH 5.57 rapidly rose to around 8.5 within a few minutes, which should be due to the release of OH^- from the fast corrosion of S/NZVI (as demonstrated in Eq. (7)). This reveals that the reaction between S/NZVI and water was fast at initial pH of 5.57, which might be the reason for the lower TCE dechlorination. This seems to be contrary to the findings of Han and Yan (2016), in which the reactivity of S/NZVI is contaminant-specific and is selective against the background reaction of water reduction. The controversy might result from the different initial pH employed in the study of Han and Yan (2016), in which the experiments were carried out at initial pH of 7.8–8.2. In this study, it was also found that more efficient TCE dechlorination was obtained at pH 8.02 than pH 5.57. Bulter and Hayes (2001) reported that the rate of TCE degradation by FeS increased with increase of pH from 7.3 to 9.3, which was possibly due to a decrease in the reduction potential of reactive surface species with increasing pH. It was also reported that the deprotonated ligands (i.e., $\equiv FeO^-$ and $\equiv S^-$) are more favorable for electron donation (Kim et al., 2013), which results in the increased rates of TCE reduction at higher pH levels.

3.3. Effect of dissolved oxygen

In the real application, the lifetime of NZVI would be significantly influenced by the existence of oxidizing substances (e.g., dissolved oxygen (DO)) in the aqueous environment. The presence of DO can cause rapid oxidation of NZVI, resulting in a loss of reactivity towards contaminants (Dong et al., 2016b). In order to verify if the coated FeS shell could relieve the oxidation of NZVI by DO, the effect of DO on TCE removal by S/NZVI was examined and the results are shown in Fig. 6A. As for S/NZVI, although the removal rate of TCE was slightly slower in air-water environment than that in air stripping-water environment at the beginning of the reaction, there was no difference in the total removal efficiency after 6 h of reaction. However, under the same circumstance, the removal efficiency of TCE by NZVI decreased from 79% (without DO) to 58% (with DO). To further explore the influence of DO on the degradation of TCE, the dechlorination efficiency was examined. As shown in Fig. 6B, in the S/NZVI reaction system, the dechlorination was significantly inhibited in the first 2 h of reaction under air condition. However, there was only a slight decrease in dechlorination efficiency under air condition than that under air-stripping condition at the end of the reaction. It was presumed that the inhibition of dechlorination at the outset of experiments might be due to the competition between DO and TCE for reaction with S/NZVI. Yet, the fact that the final dechlorination efficiency was slightly influenced by DO reveals that although S/NZVI could not be selective against reaction with DO, the presence of FeS layer might be able to alleviate the surface passivation of NZVI caused by DO oxidation. To approve this, the corrosion of S/NZVI in the absence and presence of DO was compared with that of NZVI by monitoring the variation of oxidation-reduction potential (ORP) during the reactions (Fig. 6C). It was found that the ORP value decreased sharply to around −700 eV in the S/NZVI systems under both air-

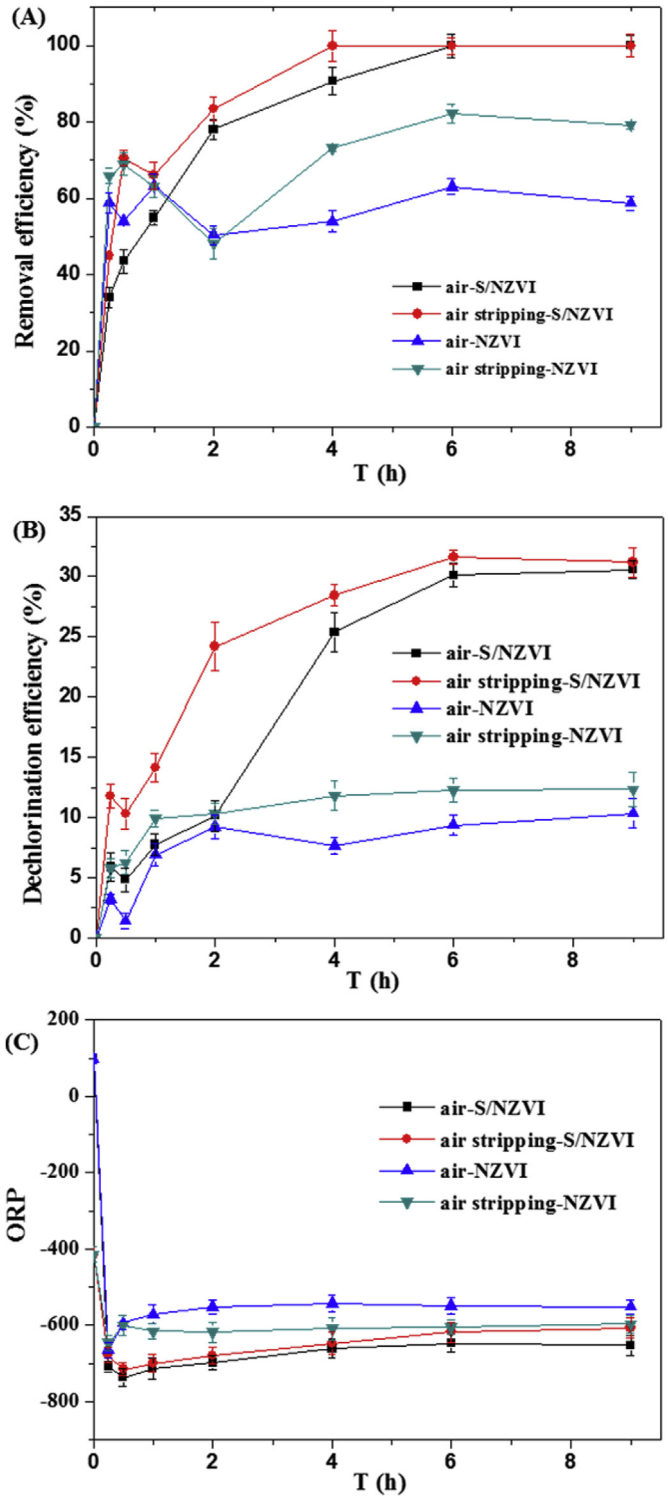

Fig. 6. (A) TCE removal and (B) TCE dechlorination by NZVI and S/NZVI in the presence and absence of dissolved oxygen, and (C) the variation of ORP during the reactions. (Fe/S = 60, TCE = 30 mg/L, NZVI=S/NZVI = 5 g/L, pH = 5.57).

stripping condition and air condition. As for the NZVI system, the ORP value also decreased sharply to around −600 eV under air-stripping or air condition. The drop of ORP in S/NZVI system was more than that in NZVI system, suggesting a higher degree of corrosion of S/NZVI than NZVI. This further reveals that S/NZVI had stronger anti-passivation ability than NZVI. Thus, it can be presumed that the sulfidation of NZVI could not avoid the side reaction with DO, but could possibly alleviate the surface passivation of NZVI caused by oxidation. This resulted in a higher reactivity of S/NZVI towards TCE than the bare NZVI.

In addition, it has been reported that the free radicals such as $^{\cdot}O_2^-$ and $^{\cdot}OH$ derived from dissolved molecular oxygen could be yielded in the S/NZVI system (Eqs. (10)–(12)) (Song et al., 2016), which could facilitate the elimination of TCE (Beltrán et al., 1996).

$$\equiv Fe - S - Fe^{2+} + O_{2,ad} \rightarrow \equiv Fe - S - Fe^{3+} + {}^{\cdot}O_2^- \quad (10)$$

$$\equiv Fe^{2+} + {}^{\cdot}O_2^- + 2H^+ \rightarrow \equiv Fe^{3+} + H_2O_2 \quad (11)$$

$$Fe^{2+} + H_2O_2 \rightarrow Fe^{3+} + {}^{\cdot}OH + OH^- \quad (12)$$

Overall, it can be seen that the presence of DO exerted more influence on the NZVI system than the S/NZVI system. This verifies that the sulfidation of NZVI could alleviate the negative impact of DO on the reactivity of NZVI.

3.4. Effect of aging

To further verify whether and how the sulfidation of NZVI could alleviate the surface passivation of NZVI caused by corrosion, the S/NZVI particles were aged in water for different time and then used for TCE degradation. As demonstrated in Fig. 7A, the effect of aging time on the dechlorination of TCE by the aged S/NZVI was determined. It was found that S/NZVI aged for 10–20 d still kept a high capacity of TCE dechlorination compared with the fresh S/NZVI, whereas an obvious drop in TCE dechlorination was observed for S/NZVI aged for 30 d. The dechlorination efficiency of TCE by freshly-prepared S/NZVI was 31.2%, while that of S/NZVI-10d, S/NZVI-20d and S/NZVI-30d were 30%, 27.5% and 23%, respectively. Previous studies have shown that the reactivity of NZVI towards contaminants could be rapidly reduced after aging for just several days due to serious surface passivation caused by corrosion (Kim et al., 2010; Dong et al., 2016b). In comparison, it was clear that the sulfidation of NZVI did prolong its lifetime.

Given that the reactivity of S/NZVI was directly associated with the surface composition (Kim et al., 2014), XRD analysis was then conducted to identify the composition evolution of S/NZVI with aging time (Fig. 7B). Fig. 7B shows the XRD patterns of fresh NZVI and S/NZVI, which indicate the presence of Fe^0 ($2\Theta = 44.6^\circ$) in S/NZVI, just like NZVI (Dong et al., 2016b). However, no iron sulfide peak is observed. Similar phenomenon was also observed in other studies (Kim et al., 2011; Su et al., 2015). The peaks of iron sulfide in the fresh S/NZVI could not be discerned in the pattern, which might be due to their low concentrations or low degree of crystallinity, or the overlapping with the peak of Fe^0 (Kim et al., 2011; Fan et al., 2014). For the aged samples, some peaks assigned to iron oxide and iron sulfide appeared, indicating the chemical and structural transformation of S/NZVI with aging. The peaks "L" and "N" at 35° and 30°, 54°, 56° in the aged S/NZVI represent lepidocrocite (γ-FeOOH) and magnetite/maghemite (Fe_3O_4/γ-Fe_2O_3), respectively (Dong et al., 2018). Another major peak "M" at 22°, 41°, 68° represents the existence of ferrous sulfide (FeS) and the minor peaks "P" and "G" at 43° and 33° represent pyrite (FeS_2) and greigite (Fe_3S_4), respectively (He et al., 2010). With the increase of aging time, the peak of Fe^0 receded, and the peaks of FeS, FeS_2 and Fe_3S_4 became obvious. Even though, there was still obvious peak of Fe^0 in the S-NZVI aged for 10–20 d. However, in the S/NZVI aged for 30 d, the peak of Fe^0 disappeared and the peaks of γ-FeOOH and Fe_3O_4/γ-Fe_2O_3 increased rapidly. The reduction of Fe^0 content and the accumulation of iron oxides should be the reason for the decreased

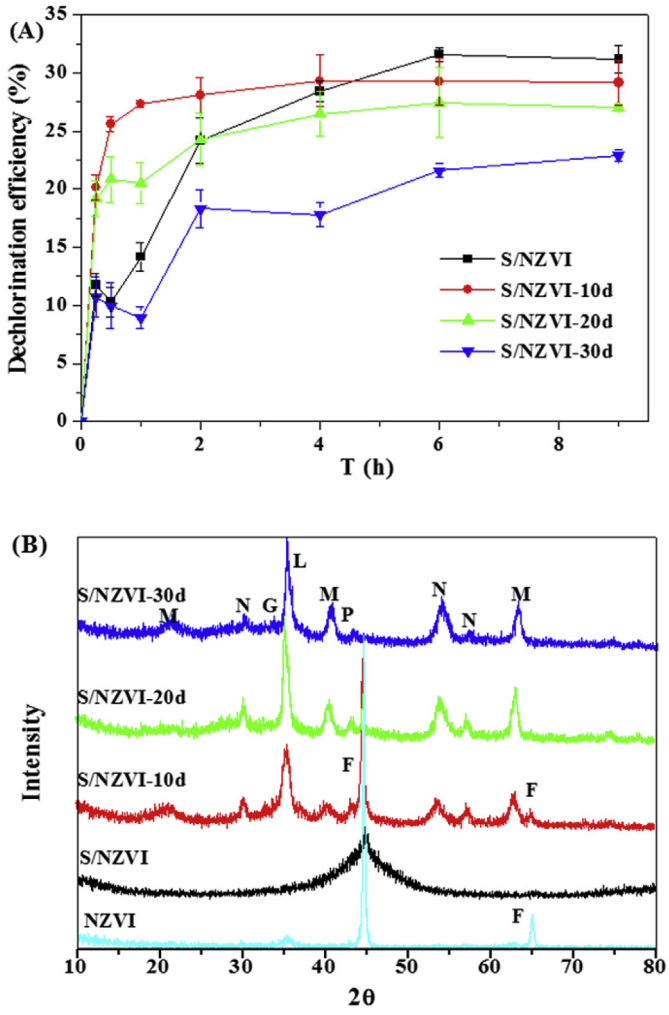

Fig. 7. (A) Effect of particle aging on the dechlorination of TCE by S/NZVI (Fe/S = 60, TCE = 30 mg/L, S/NZVI = 5 g/L, pH = 5.57); (B) XRD analysis of NZVI, S/NZVI and aged-S/NZVI nanoparticles. Peaks refer to Fe^0 (F), lepidocrocite (γ-FeOOH) (L), magnetite/maghemite (Fe_3O_4/γ-Fe_2O_3) (N), ferrous sulfide (FeS)(M), pyrite (FeS_2) (P), greigite (Fe_3S_4)(G).

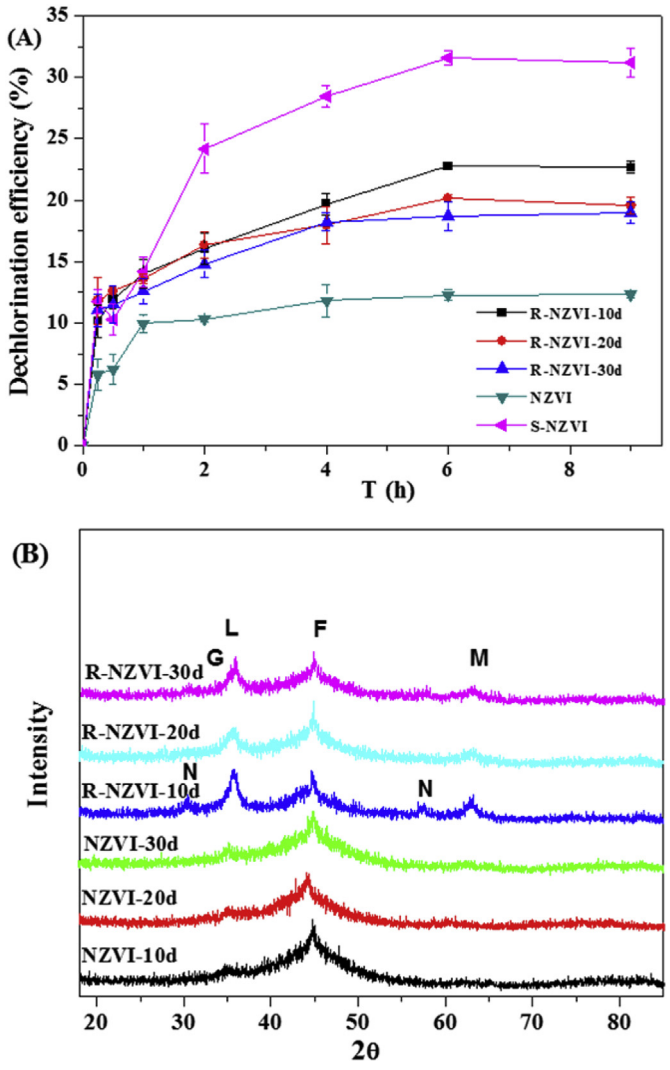

Fig. 8. (A) Dechlorination of TCE by the sulfur-reactivated aged-NZVI (R-NZVI) (Fe/S = 60, TCE = 30 mg/L, NZVI=S/NZVI = R-NZVI = 5 g/L); (B) XRD analysis of aged-NZVI and sulfur-reactivated aged-NZVI. Peaks refer to Fe^0 (F), lepidocrocite (γ-FeOOH) (L), magnetite/maghemite (Fe_3O_4/γ-Fe_2O_3) (N), ferrous sulfide (FeS) (M), greigite (Fe_3S_4)(G).

dechlorination efficiency of the aged S/NZVI, especially for S/NZVI-30d. Nevertheless, although the iron oxides (e.g., γ-FeOOH and Fe_3O_4/γ-Fe_2O_3) were accumulated on the surface of S/NZVI-30d, the dechlorination efficiency of S/NZVI-30d still reached a higher level (23%) compared with that of fresh-prepared NZVI (12.3%). This should be attributed to the excellent electron conductivity of FeS on the particle surface (Butler and Hayes, 2001).

3.5. Reactivation of aged NZVI by sulfidation

In real application, NZVI particles are usually synthesized on site during the site remediation to avoid oxidation; otherwise, the particles can be easily passivated and lose reactivity during long-term storage (Dong et al., 2016a; Liang et al., 2014; Qin et al., 2017). For the aged NZVI, previous studies have developed various methods (e.g., acid washing, H_2-pretreatment, ultrasound, premagnetization) to reactivate its reactivity before the application (Guan et al., 2015; Li et al., 2015; Sun et al., 2017). In this study, we tried to examine whether the sulfidation with $Na_2S_2O_4$ could reactivate the aged NZVI. As shown in Fig. 8A, the dechlorination of TCE by the $Na_2S_2O_4$-reactivated aged NZVI (R-NZVI) were measured and compared with that of fresh S/NZVI and fresh NZVI. The results show that although the dechlorination efficiency of R-NZVI was still not comparable to that of S/NZVI, but was superior to that of fresh NZVI. Besides, it was found that the aging time of NZVI had limited influence on the reactivation of NZVI by sulfidation. The dechlorination efficiency by R-NZVI decreased slightly with the increase of aging time of NZVI, reaching 23%, 20%, and 19% with aging time of 10 d, 20 d, and 30 d, respectively. The results suggest that sulfidation with $Na_2S_2O_4$ could be a feasible way for the reactivation of aged NZVI for the degradation of TCE.

In addition, the chemical composition of aged NZVI and R-NZVI were further analyzed by XRD (Fig. 8B). The XRD pattern of aged NZVI shows the existence of Fe^0 and small amount of iron oxides. A comparison of XRD patterns of NZVI with different aging time indicates that the peak of Fe^0 became weaker with the increase of aging time. When $Na_2S_2O_4$ was added to reactivate the aged NZVI, the peaks of ferrous sulfide (FeS), greigite (Fe_3S_4) and lepidocrocite (γ-FeOOH) appeared. Thus, the presence of FeS on the surface of R-NZVI should contribute to the enhanced dechlorination of TCE compared with fresh NZVI. However, the reactivity of R-NZVI was still not as good as S/NZVI, which should be due to the presence of

iron oxides (e.g., γ-FeOOH) on the surface of R-NZVI and the less content of Fe^0.

4. Conclusion

In this study, we investigated the effects of Fe/S molar ratio, pH, dissolved oxygen (DO) and particle aging on TCE degradation by S/NZVI. The following conclusions were made:

- Fe/S ratio greatly affected the dechlorination efficiency of TCE by S/NZVI. The TCE dechlorination efficiency achieved the maximum value at Fe/S molar ratio of ~60, and it decreased at both higher and lower Fe/S. The spectroscopic analysis reveal that the presence of FeS formed on the surface of NZVI played a key role in the dechlorination process.
- The increasing solution pH from ~5 to ~8 significantly increased TCE degradation by S/NZVI. This suggests that S/NZVI would be an efficient reagent for the remediation of groundwater (with typical pH ~ 8).
- The presence of DO and the aging time of S/NZVI had limited effect on TCE dechlorination efficiency. The results reveal that the presence of FeS layer could be able to alleviate the surface passivation of NZVI caused by corrosion, prolonging the lifetime of S/NZVI.
- The feasibility of reactivation of the aged NZVI by sulfidation treatment was examined. It was found the reactivated NZVI even had higher reactivity than the fresh NZVI. XRD analysis shows that FeS was generated on the surface of the aged NZVI after sulfidation, which should contribute to the improved reactivity. This reveals that sulfidation treatment could be a feasible way for the reactivation of aged NZVI.

Acknowledgements

This research was supported by the National Natural Science Foundation of China (51409100, 51521006), the Fundamental Research Funds for the Central Universities (531107040788), and the Program for Changjiang Scholars and Innovative Research Team in University (IRT-13R17).

Appendix A. Supplementary data

Supplementary data related to this article can be found at https://doi.org/10.1016/j.watres.2018.02.017.

References

Ahmad, M., Lee, S.S., Dou, X., Mohan, D., Sung, J.K., Yang, J.E., Ok, Y.S., 2012. Effects of pyrolysis temperature on soybean stover- and peanut shell-derived biochar properties and TCE adsorption in water. Bioresour. Technol. 118, 536–544.
Arnold, W.A., Roberts, A.L., 2000. Pathways and kinetics of chlorinated ethylene and chlorinated acetylene reaction with Fe(0) particles. Environ. Sci. Technol. 34 (9), 1794–1805.
Beltrán, F.J., González, M., Acedo, B., Jaramillo, J., 1996. Contribution of free radical oxidation to eliminate volatile organochlorine compounds in water by ultraviolet radiation and hydrogen peroxide. Chemosphere 32 (10), 1949–1961.
Butler, E.C., Hayes, K.F., 2001. Factors influencing rates and products in the transformation of trichloroethylene by iron sulfide and iron metal. Environ. Sci. Technol. 35 (19), 3884.
Chen, J.L., Al-Abed, S.R., Ryan, J.A., Li, Z.B., 2001. Effects of pH on dechlorination of trichloroethylene by zero-valent iron. J. Hazard Mater. 83 (3), 243–254.
Chernyshova, I.V., 2003. An in situ FTIR study of galena and pyrite oxidation in aqueous solution. J. Electroanal. Chem. 558, 83–98.
Dong, H.R., Zeng, Y., Zeng, G., Huang, D., Liang, J., Zhao, F., He, Q., Xie, Y., Wu, Y., 2016a. EDDS-assisted reduction of Cr(VI) by nanoscale zero-valent iron. Separ. Purif. Technol. 165, 86–91.
Dong, H., Zhao, F., Zeng, G., Tang, L., Fan, C., Zhang, L., Zeng, Y., He, Q., Xie, Y., Wu, Y., 2016b. Aging study on carboxymethyl cellulose-coated zero-valent iron nanoparticles in water: chemical transformation and structural evolution. J. Hazard Mater. 312, 234.
Dong, H.R., He, Q., Zeng, G.M., Tang, L., Zhang, L.H., Xie, Y.K., Zeng, Y.L., Zhao, F., 2017a. Degradation of trichloroethene by nanoscale zero-valent iron (nZVI) and nZVI activated persulfate in the absence and presence of EDTA. Chem. Eng. J. 316, 410–418.
Dong, H.R., Zhang, C., Hou, K.J., Cheng, Y.J., Deng, J.M., Jiang, Z., Tang, L., Zeng, G.M., 2017b. Removal of trichloroethylene by biochar supported nanoscale zero-valent iron in aqueous solution. Separ. Purif. Technol. 188, 188–196.
Dong, H.R., Zhao, F., He, Q., Xie, Y.K., Zeng, Y.L., Zhang, L.H., Tang, L., Zeng, G.M., 2017c. Physicochemical transformation of carboxymethyl cellulose-coated zero-valent iron nanoparticles (nZVI) in simulated groundwater under anaerobic conditions. Separ. Purif. Technol. 175, 376–383.
Dong, H.R., Jiang, Z., Deng, J.M., Zhang, C., Cheng, Y.J., Hou, K.J., Zhang, L.H., Tang, L., Zeng, G.M., 2018. Physicochemical transformation of Fe/Ni bimetallic nanoparticles during aging in simulated groundwater and the consequent effect on contaminant removal. Water Res. 129, 51–57.
Fan, D.M., Anitori, R.P., Tebo, B.M., Tratnyek, P.G., 2014. Oxidative remobilization of technetium sequestered by sulfide-transformed nano zerovalent iron. Environ. Sci. Technol. 48, 7409–7417.
Gao, J., Wang, W., Rondinone, A.J., He, F., Liang, L., 2015. Degradation of trichloroethene with a novel ball milled Fe-C nanocomposite. J. Hazard Mater. 300, 443–450.
Garcia, A.N., Boparai, H.K., O'Carroll, D.M., 2016. Enhanced dechlorination of 1,2-dichloroethane by coupled nano iron-dithionite treatment. Environ. Sci. Technol. 50, 5243–5251.
Guan, X.H., Sun, Y., Qin, H., Li, J., Lo, I.M.C., He, D., Dong, H.R., 2015. The limitations of applying zero-valent iron technology in contaminants sequestration and the corresponding countermeasures: the development in zero-valent iron technology in the last two decades (1994-2014). Water Res. 75, 224–248.
Han, Y., Yan, W., 2016. Reductive dechlorination of trichloroethene by zero-valent iron nanoparticles: reactivity enhancement through sulfidation treatment. Environ. Sci. Technol. 50 (23), 12992–13001.
Hansson, E.B., Odziemkowski, M.S., Gillham, R.W., 2008. Influence of Na2S on the degradation kinetics of CCl4 in the presence of very pure iron. J. Contam. Hydrol. 98 (3), 128–134.
He, Y.T., Wilson, J.T., Wilkin, R.T., 2010. Impact of iron sulfide transformation on trichloroethylene degradation. Geochim. Cosmochim. Acta 74, 2025–2039.
Jeong, H.Y., Han, Y.S., Park, S.W., Hayes, K.F., 2010. Aerobic oxidation of mackinawite (FeS) and its environmental implication for arsenic mobilization. Geochim. Cosmochim. Acta 74 (11), 3182–3198.
Khalil, A.M.E., Eljamal, O., Jribi, S., Matsunaga, N., 2016. Promoting nitrate reduction kinetics by nanoscale zero valent iron in water via copper salt addition. Chem. Eng. J. 287, 367–380.
Kim, E.J., Kim, J.H., Chang, Y.S., Azad, A.M.D., Chang, Y.S., 2011. Facile synthesis and characterization of Fe/FeS nanoparticles for environmental applications. ACS Appl. Mater. Interfaces 3 (5), 1457–1462.
Kim, E.J., Kim, J.H., Chang, Y.S., Turcio-Ortega, D., Tratnyek, P.G., 2014. Effects of metal ions on the reactivity and corrosion electrochemistry of Fe/FeS nanoparticles. Environ. Sci. Technol. 48 (7), 4002–4011.
Kim, E.J., Murugesan, K., Kim, J.H., Tratnyek, P.G., Chang, Y.S., 2013. Remediation of trichloroethylene by FeS-coated iron nanoparticles in simulated and real groundwater: effects of water chemistry. Ind. Eng. Chem. Res. 52 (27), 9343–9350.
Kim, H.S., Ahn, J.Y., Hwang, K.Y., Kim, I.K., Hwang, I., 2010. Atmospherically stable nanoscale zero-valent iron particles formed under controlled air contact: characteristics and reactivity. Environ. Sci. Technol. 44 (5), 1760–1766.
Li, J.X., Qin, H.J., Guan, X.H., 2015. Premagnetization for enhancing the reactivity of multiple zerovalent iron samples toward various contaminants. Environ. Sci. Technol. 49 (24), 14401–14408.
Lee, W., Batchelor, B., 2002. Abiotic reductive dechlorination of chlorinated ethylenes by iron-bearing soil minerals. 1. Pyrite and magnetite. Environ. Sci. Technol. 36 (23), 5147–5154.
Liu, Y., Majetich, S.A., Tilton, R.D., Sholl, D.S., Lowry, G.V., 2005. TCE dechlorination rates, pathways, and efficiency of nanoscale iron particles with different properties. Environ. Sci. Technol. 39 (5), 1338–1345.
Liang, L.P., Sun, W., Guan, X.H., Huang, Y.Y., Choi, W.Y., Bao, H.L., Li, L.N., Jiang, Z., 2014. Weak magnetic field significantly enhances selenite removal kinetics by zero valent iron. Water Res. 49, 371–380.
Matheson, L.J., Tratnyek, P.G., 1994. Reductive dehalogenation of chlorinated methanes by iron metal. Environ. Sci. Technol. 28 (12), 2045–2053.
Qin, H.J., Li, J.X., Yang, H.Y., Pan, B.C., Zhang, W.M., Guan, X.H., 2017. The coupled effect of ferrous ion and oxygen on the electron selectivity of zerovalent iron for selenate sequestration. Environ. Sci. Technol. 51, 5090–5097.
Rajajayavel, S.R.C., Ghoshal, S., 2015. Enhanced reductive dechlorination of trichloroethylene by sulfidated nanoscale zero valent iron. Water Res. 78, 144–153.
Reyes-Bozo, L., Escudey, M., Vyhmeister, E., Higueras, P., Godoy-Faúndez, A., Salazar, J.L., Valdés-González, H., Wolf-Sepúlveda, G., Herrera-Urbina, R., 2015. Adsorption of biosolids and their main components on chalcopyrite, molybdenite and pyrite: zeta potential and FTIR spectroscopy studies. Miner. Eng. 78, 128–135.
Su, Y., Adeleye, A.S., Keller, A.A., Huang, Y., Dai, C., Zhou, X., Zhang, Y., 2015. Magnetic sulfide-modified nanoscale zerovalent iron (S-nZVI) for dissolved metal ion removal. Water Res. 74, 47–57.
Sun, Y.K., Hu, Y.H., Huang, T.L., Li, J.X., Qin, H.J., Guan, X.H., 2017. Combined effect of weak magnetic fields and anions on arsenite sequestration by zerovalent iron:

kinetics and mechanisms. Environ. Sci. Technol. 51 (7), 3742–3750.
Seyama, T., Adachi, K., Yamazaki, S., 2012. Kinetics of photocatalytic degradation of trichloroethylene in aqueous colloidal solutions of TiO_2 and WO_3 nanoparticles. J. Photochem. Photobiol. Chem. 249 (23), 15–20.
Shao, H.B., Butler, E.C., 2009. The relative importance of abiotic and biotic transformation of carbon tetrachloride in anaerobic soils and sediments. Soil Sediment Contam. 18, 455–469.
Song, S., Su, Y., Adeleye, A.S., Zhang, Y., Zhou, X., 2016. Optimal design and characterization of sulfide-modified nanoscale zerovalent iron for diclofenac removal. Appl. Catal. B Environ. 201, 211–220.
Stroo, H.F., Unger, M., Ward, C.H., Kavanaugh, M.C., Vogel, C., Leeson, A., Marqusee, J., Smith, B.P., 2003. Remediating chlorinated solvent source zones. Environ. Sci. Technol. 37 (11), 224A–230A.
Utsumi, S., 2006. New colorimetric determination of chloride using mercuric thiocyanate and ferric ion. Bull. Chem. Soc. Jpn. 25 (3), 226–226.
Wang, C.B., Zhang, W., 1997. Synthesizing nanoscale iron particles for rapid and complete dechlorination of TCE and PCBs. Environ. Sci. Technol. 94 (18), 9602–9607.
Wei, Z., Seo, Y., 2010. Trichloroethylene (TCE) adsorption using sustainable organic mulch. J. Hazard Mater. 181 (1–3), 147–153.
Weir, B.A., Mclane, C.R., Leger, R.J., 2010. Design of a UV oxidation system for treatment of TCE-contaminated groundwater. Environ. Prog. 15 (3), 179–186.
Xie, Y.K., Dong, H.R., Zeng, G.M., Tang, L., Jiang, Z., Zhang, C., Deng, J.M., Zhang, L.H., Zhang, Y., 2017. The interactions between nanoscale zero-valent iron and microbes in the subsurface environment: a review. J. Hazard Mater. 321, 390–407.
Yan, J., Han, L., Gao, W., Xue, S., Chen, M., 2015. Biochar supported nanoscale zerovalent iron composite used as persulfate activator for removing trichloroethylene. Bioresour. Technol. 175, 269–274.
Yamashita, T., Hayes, P., 2008. Analysis of XPS spectra of Fe^{2+} and Fe^{3+} ions in oxide materials. Appl. Surf. Sci. 254, 2441–2449.